Journal of Magnetism and Magnetic Materials 458 (2018) 66–74

Contents lists available at ScienceDirect

Journal of Magnetism and Magnetic Materials

journal homepage: www.elsevier.com/locate/jmmm

Research articles

A new $Sm(Co,Fe,Cu)_4B/Sm_2(Co,Fe,Cu)_7$ cell structure with the coercivity of up to 5.01 T

Xiang Chi, Ying Li, Xu-hao Han, Xiu-li Duan, Ji-bing Sun *, Chun-xiang Cui

Key Lab. for new type of functional materials in Hebei Province, Hebei University of Technology, No.1 Dingzigu Road, Hongqiao District, Tianjin 300130, PR China

A R T I C L E I N F O

Article history:
Received 23 November 2017
Received in revised form 14 February 2018
Accepted 3 March 2018
Available online 5 March 2018

Keywords:
Rare earth alloys and compounds
Microstructure
Atomic scale structure
EXAFS
Magnetic properties

A B S T R A C T

A new $Sm(Co,Fe,Cu)_4B/Sm_2(Co,Fe,Cu)_7$ cell structure is found, and its phase composition, microstructure and magnetic properties are investigated. Particularly, the atom structure of main phase is analyzed by extended X-ray absorption fine structure. It was found that as-spun $SmCo_{2.94}FeCu_{0.06}B$ ribbons were composed of amorphous phase and approximate equiaxed $Sm(Co,Fe,Cu)_4B$ nanocrystallines. The high disorder of the nanocrystallines leads to the low magnetic anisotropy. After the as-spun ribbons were annealed at 800 °C for 30 min, the amorphous phase disappeared completely. The short rod-shaped $Sm(Co,Fe,Cu)_4B$ grains have a staggered distribution accompanied by ~8 vol% lamellar $Sm_2(Co,Fe,Cu)_7$ phase at grain boundaries, and the new cell/cell-wall-type $Sm(Co,Fe,Cu)_4B/Sm_2(Co,Fe,Cu)_7$ microstructure is produced. The annealed ribbons show an ultra-high coercivity of up to 5.01 T at room temperature, 40.64 T at 5 K (obtained by extrapolating), and estimated to be ~ 41.96 T at 0 K. The microstructureal models of both ribbons are created and the coercivity mechanism is discussed in detail.

1. Introduction

Nowadays, three generations of permanent magnets, i.e., $SmCo_5$, Sm_2Co_{17} and Nd-Fe-B, have been greatly developed and widely applied in these fields such as electric motors and generators, electroacoustics, computer peripherals, medical equipment and magnetomechanics, etc [1]. Among these materials, Nd-Fe-B magnets possess the highest magnetic energy product, while the Sm-Co magnets have an advantage of application in high temperature environments [2,3]. In Sm-Co alloys, $SmCo_5$-based alloys have been widely exploited for application due to their characteristics of high magnetic energy product, high coercivity and strong anisotropy, and excellent temperature stability [4].

Téllez-Blanco et al. [5] showed that the coercivity of annealed $SmCo_{5-x}Cu_x$ (x = 1, 1.5, 2, 2.5, 3, 4) alloys first increased, then reached a maximum of 2.08_MA/m at x = 2.5, and finally decreased with the increase of x. Zhang et al. [6] found that the coercivity enhancement in $SmCo_{4.5}$/Cu multilayer film could be attributed to the formation of the $Sm(Co,Cu)_5$ phase with high magnetic anisotropy when Cu was incorporated into the $SmCo_5$. In the case of a small addition of Cu into $SmCo_5$, Cu prefers to substitute for Co at 2c site and thus the $Sm(Co,Cu)_5$ phase will form [7]. Therefore, the appropriate addition of Cu into $SmCo_5$ can lead to a magnetic hardening and the change of magnetization orientation, and ultimately improve the coercivity of $Sm(Co,Cu)_5$ alloy. However, too much Cu addition will weaken the magnetocrystalline anisotropy field and consequently reduce the coercivity of $SmCo_{5-x}Cu_x$. On the other hand, the Cu doping will partly give rise to the weak exchange interaction between Sm and Cu atoms instead of the strong 3d-4f exchange interaction between Sm and Co atoms, resulting in a decrease in the total magnetic moment [8].

In addition, the substitution of B for Co in $SmCo_5$ phase produces the $R_{1+n}Co_{5+3n}B_{2n}$-type structures, which are formed by stacking one-layer $SmCo_5$ and n-layer RCo_3B_2 along the c-axis [9]. A giant magnetocrystalline anisotropy can be produced in Sm-Co-B alloys with the $R_{1+n}Co_{5+3n}B_{2n}$-type structures, especially such as $SmCo_4B$ with $CeCo_4B$-type hexagonal structure and space group P6/mmm, which has a very high anisotropy field up to 120 T at 4.2 K, much larger than 71 T of $SmCo_5$. However, the Curie temperature (T_c) and magnetization of $SmCo_4B$ are both lower than those of $SmCo_5$ [10,11]. Furthermore, the substitution of Fe for Co in $SmCo_4B$ can lead to formation of $SmCo_{4-x}Fe_xB$ phase, which has a higher anisotropic field and magnetization than $SmCo_4B$ [12]. But, owing to the limited solubility of Fe in the $SmCo_{4-x}Fe_xB$ phase, the single $Sm(Co,Fe)_4B$ phase is obtained when x < 1, while two phases of $Sm(Co,Fe)_4B$ and $Sm_2(Co,Fe)_{17}B_y$ coexist in $SmCo_{4-x}Fe_xB$ alloys for x ≥ 1 [13]. Jiang et al. [14] reported that after as-spun $SmCo_{4-x}Fe_xB$ ribbons were annealed at 800 °C for 30 min, the total magnetization of the annealed ribbons increased by about 24% at x = 2 while their coercivity first increased, reached a maximum of

* Corresponding author.
E-mail address: hbgdsjb@hebut.edu.cn (J.-b. Sun).

https://doi.org/10.1016/j.jmmm.2018.03.007
0304-8853/

about 44 kOe at $x = 1$, and then decreased with increasing x. The continuous raise of Fe content will form a new $Sm_2(Co,Fe)_{17}B_y$ phase, whose anisotropic field is smaller compared to the $Sm(Co,Fe)_4B$ phase, and therefore the coercivity of ribbons decreases.

Based on the high anisotropy field of the $SmCo_4B$ phase and $SmCo_{4-x}Fe_xB$ phase is produced from $SmCo_5$, we predict that the $SmCo_{4-x}Cu_xB$ alloys should have a higher coercivity but simultaneously the solid solution of Cu in $SmCo_4B$ may reduce its magnetization. In this work, we prepare a new $SmCo_{2.94}FeCu_{0.06}B$ alloy by doping Cu into the $SmCo_{4-x}Fe_xB$ with an aim of further improving the coercivity of $SmCo_{4-x}Fe_xB$ alloys. Furthermore, the atomic structure of the $SmCo_{2.94}FeCu_{0.06}B$ is analyzed by utilizing the extended X-ray absorption fine structure (EXAFS) method in order to explain the reason why it has an ultra-high coercivity.

2. Experimental

The as-spun ribbons with a nominal composition $SmCo_{2.94}FeCu_{0.06}B$ were prepared by using pure Sm, Co, Fe, Cu and B by arc-melting, accompanied with melt-spinning with a tangential wheel velocity of 40 m/s in high purity argon at a chamber pressure of 0.6×10^5 Pa. Meanwhile, extra 10 wt% Sm was added to compensate for the vaporization of Sm during the arc-melting and melt-spinning. Then, a part of as-spun ribbons were annealed at 800 °C for 30 min to obtain the annealed ribbons. Subsequently, a part of the as-spun and annealed ribbons were ground into powder in ethanol.

The phase compositions of both powders were analyzed by using a Rigaku Dmax 2500 Pc X-ray diffractometer (XRD) with Cu K_α radiation and a graphite monochromator. The microstructures of both ribbons were observed by TECNAI G^2 F20 high resolution transmission electron microscopy (HRTEM). The ribbon samples for the TEM observation were prepared by ion milling. The magnetic properties of as-spun and annealed ribbons were measured by LakeShore 7407 vibrating sample magnetometer (VSM) with a maximum field of 2 T and Dyna Cool physical property measurement system (PPMS) with a maximum field of 9 T, respectively. In order to obtain the credible coercivity performance, the as-spun ribbons were magnetized by a 5 T peak pulse field before the VSM measurement. The EXAFS experiments were performed at the 4B9A beamline of the Beijing Synchrotron Radiation Facility (BSRF). The storage ring ran at 2.5 GeV with a maximum electron current of about 250 mA. The energy range of the incident X-ray was tunable from 4 to 25 keV by fix-exit Si (1 1 1) double crystal monochromator. The absorption edge of standard metal foils was used to calibrate the X-ray energy. Samples were ground into fine powers and then smeared on Scotch tapes. Sm L_3-edge (6716 eV) EXAFS spectra were collected at energy range from 6516 eV to 7116 eV at RT in transmission mode using ionization chamber detectors.

3. Results and discussion

3.1. XRD analysis

Fig. 1 shows the XRD patterns of $SmCo_{2.94}FeCu_{0.06}B$ as-spun and annealed ribbons. The as-spun ribbons are mainly composed of $CeCo_4B$-type $Sm(Co,Fe,Cu)_4B$ (for short 1:4:1) phase, as shown in Fig. 1a. This indicates that Fe and Cu atoms occupy the Co sites in the $SmCo_4B$ phase, leading to the formation of the 1:4:1 solid solution phase. Many amorphous diffuse scattering peaks and hill-like amorphous peaks at the bottom of the high-intensity diffraction peaks are also observed in the as-spun ribbons. This is due to the fact that the diffusion of atoms is suppressed at an extremely fast cooling rate during the melt-spinning process, which favors the formation of amorphous phase. Besides, the alloys with the solid solution of Fe and Cu meet more easily three principles of amorphous formation proposed by Inoue [15], and therefore the amorphous phase can form in the as-spun ribbons.

From Fig. 1b one can see that the annealed ribbons are composed of 1:4:1 phase and a small amount of Ce_2Ni_7-type $Sm_2(Co,Fe,Cu)_7$ (for short 2:7) phase. Simultaneously, in Fig. 1b, both the degree of diffuse scattering and the hill-like amorphous feature decline obviously, and the background noise does not look so thick and dark, which implies that the amorphous phase almost disappears. This is because that the amorphous phase crystallizes to form 1:4:1 and 2:7 phases during the annealing process. In comparison with the as-spun ribbons, there is a large increase in the

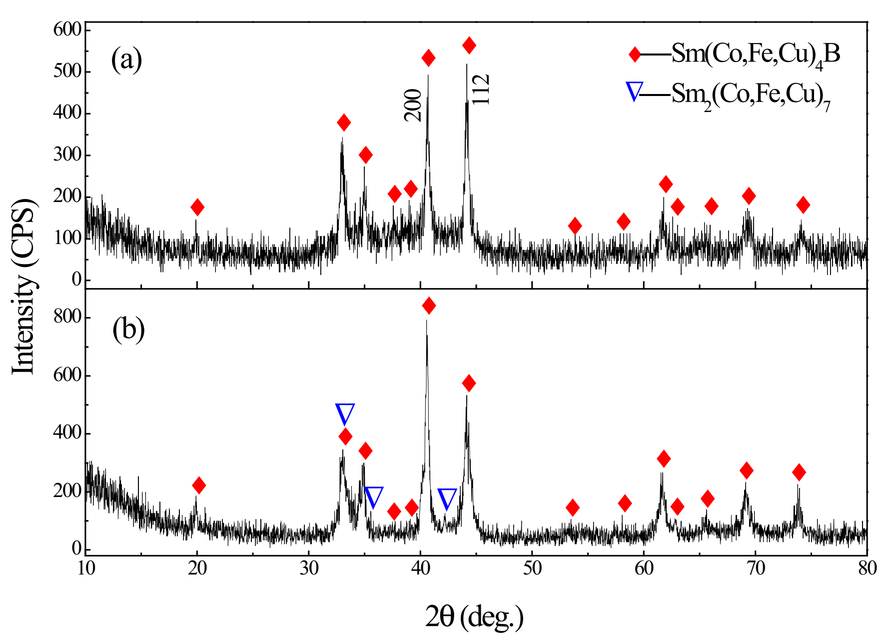

Fig. 1. XRD patterns of $SmCo_{2.94}FeCu_{0.06}B$ as-spun (a) and annealed (b) ribbons.